ISSN 0040-6015, Thermal Engineering, 2020, Vol. 67, No. 10, pp. 706–714. © Pleiades Publishing, Inc., 2020.
Russian Text © The Author(s), 2020, published in Teploenergetika.

RENEWABLE ENERGY SOURCES AND HYDROPOWER

Cogeneration Plants with Solar Radiation Concentrators

P. A. Nesterenkov[a], *, A. G. Nesterenkov[b], **, and A. N. Temirbekov[a], ***

[a] *Al-Farabi Kazakh National University, Almaty, 050040, Republic of Kazakhstan*
[b] *Chokin Kazakh Energy Research Institute, Almaty, 050012, Republic of Kazakhstan*
**e-mail: stolkner@gmail.com*
***e-mail: ionotexnica@mail.ru*
****e-mail: almas.temirbekov@kaznu.kz*

Received April 5, 2019; revised February 5, 2020; accepted March 18, 2020

Abstract—Results from experimental studies of a solar cogeneration system with linear photovoltaic modules of a fundamentally new design are presented. The Λ-shaped frontal walls are installed face-to-face at an angle to each other and mutually shield their own thermal radiation, which decreases the radiation heat losses by 27% compared with linear photovoltaic modules of the known designs. The photocurrent generated by cooled solar cells is directed to a system for charging chemical batteries and the thermal energy released is transmitted to the unconsumed intermediate heat-transfer fluid and then, through the surface of coil pipes of counter-current heat exchangers, to the consumed process water of the outer circulation circuit. The further transportation of thermal energy to the storage system occurs by natural circulation of the consumed process water through the temperature gradient formed by the control system over the height between the heat source, the heat exchanger, and the heat receiver, an insulated container (a heat accumulator). For the first time, efficient controlled transportation of heat has been implemented without using a circulation pump owing to the excess thermal energy released during the conversion of solar energy by the solar cells and a photo-selective film installed in the focal spot of the optical concentrator. Thus, a possibility of increasing the temperature of the heat-transfer fluids at the cogeneration system outlet has been offered. A two-circuit circulation system allows for separation of unconsumed heat-transfer fluids (antifreezing solutions) and the consumed fluid (the process water) by the pressure in the channels and installation of a linear counter-current heat exchanger that performs the functions of a supporting platform's mechanical axis along the rotational axis of the optical concentrator. The system uses a dual-axis solar tracking concentrating system comprised of flat mirrors installed at an angle to the horizon. The arrangement of the Λ-shaped photovoltaic modules on the supporting framework in series along the heat-transfer-fluid path allows for a reduction in the overall dimensions of the channels, an increase in the total efficiency of the solar cells, and simplification of the encapsulation technology. A method for calculating the output of the cogeneration plant is provided. The method is based on the experimentally measured characteristics of silicon solar cells and heat losses in the channels of the linear photovoltaic modules.

Keywords: silicon photovoltaic cells, optical concentrator, linear photovoltaic modules, heat exchanger, circulation system, specific output

DOI: 10.1134/S0040601520100079

The emergence on the market of relatively cheap, large-area silicon photovoltaic cells (silicon solar cells) with an efficiency of approximately 21% has incentivized the development of plants for cogeneration of electric and heat power. In 2010, T.T. Chow presented a comprehensive overview of the photovoltaic/thermal (PVT) systems with cooled photovoltaic modules [1], and J.A. Duffe and W.A. Bechman developed a method for calculating the heat exchange of fluids in the channels in 2006 [2]. A technological drawback of silicon solar cells, namely, the impossibility of heating the heat-transfer fluids to high temperatures maintaining high efficiency, impeded wide commercialization of the plants. This drawback was eliminated by the use of high-temperature CaAs photovoltaic cells and optical concentrators, which allowed for a specific electric power of approximately 170 W/m^2 and a specific heat power of approximately 530 W/m^2 to be achieved [3]. Relatively high heat losses in the photovoltaic modules (PVMs), excess generation of low-potential heat energy of little use for economic purposes, and difficulty in transporting the latter to the consumers remained a weak point of the technology [4, 5].

In this work, photovoltaic modules of a fundamentally new type are presented in which the above drawbacks have been eliminated. The concept of the technology proposed by the authors consists in the positioning of the frontal surfaces of the photovoltaic cells face-to-face in the focal spot of the optical concentrator mirrors (Λ-shaped PVMs), the connection of the

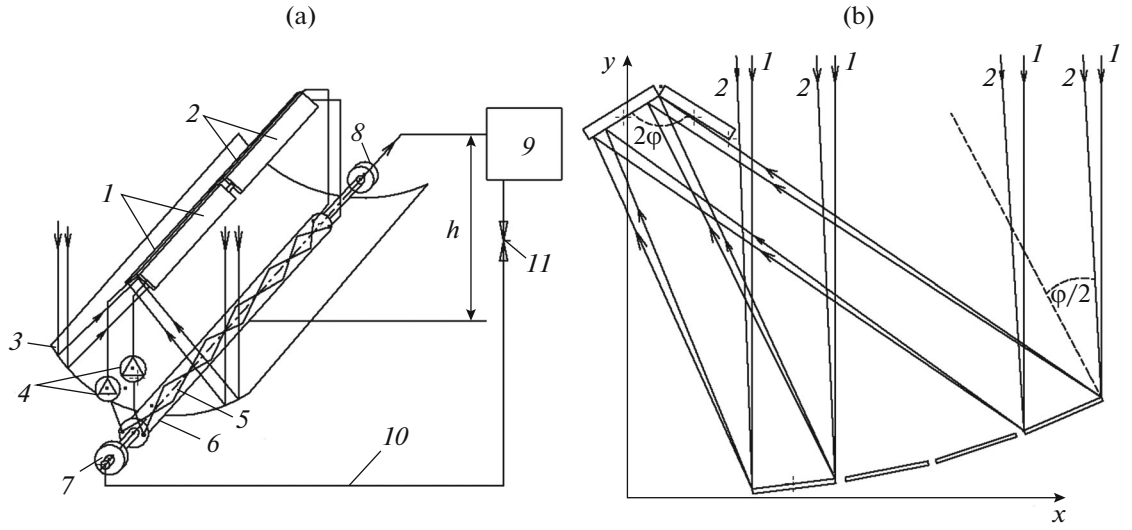

Fig. 1. Schematics of (a) the cogeneration plant and (b) the reflection of solar radiation.

PVM channels in series along the heat-transfer-fluid and photocurrent paths, and the transmission of the heat released by the solar cells to the intermediate heat-transfer fluid and then the fluid consumed in a counter-current heat exchanger. The further transportation of heat energy to a heat-insulated container is affected by natural circulation of the consumed fluid under formation of the temperature gradient in the circulation circuit.

OPTICAL SYSTEM OF THE COGENERATION PLANT

The optimal mutual alignment of linear PVMs and flat mirrors of the optical concentrator that allows for a reduction in optical losses was found by computer simulation in the environment of the Inventor software [6]. In Fig. 1, a schematic layout of the plant and the formation of solar radiation reflected by the mirrors on the solar cells are shown. Channels *1* and *2* of the cooled photovoltaic modules, the angle between the frontal walls of which equals 2φ, are placed in series in the focal spot of optical concentrator mirrors *3*. The intermediate heat-transfer fluids are pumped by pumps *4* along the solar cells and then through coil pipes *5* of counter-current heat exchanger *6*. The heat energy received by the heat-transfer fluids is transferred to the consumed fluid, which arrives through support bearings *7* and *8* owing to natural circulation to storage system *9* installed at a height *h* with respect to the heat exchanger. The circulation circuit of the heat exchanger is refilled with cold water through return pipeline *10* and valve *11*.

According to the optical scheme based on the law of solar radiation reflection and considering the geometric properties of parabolic curves, the expression for the geometric concentration K_g was obtained as follows:

$$K_g = 2\frac{f}{b}\frac{1-\cos\varphi}{1+\cos\varphi}0.5 + \frac{b_Z}{b}\cos\frac{\varphi}{2} - \left(\frac{3}{2}\sin\varphi + \frac{\delta_1}{b}\right) - \sum\frac{\delta_2}{b}, \quad (1)$$

where b and b_z are the wall and mirror widths, f is the focal distance of the parabolic surface from the frontal wall centers, δ_1 is the distance between the PVM projection onto the x axis and the first mirror, and δ_2 is the distance between the mirror edges.

At $\varphi = 50°$ and the focal distance $f = 1.8$ m, the number of the concentrator mirrors equals 12 and the geometric concentration is $K_g = 11.3$. The optical concentration C_{op} is determined by the product of three technological parameters of the concentrator as:

$$C_{op} = K_g K_r D, \quad (2)$$

where K_r is the reflection coefficient of direct solar radiation from the mirrors and D is a coefficient that considers the absorption of solar radiation in the mirrors and shielding glass.

The concentrators proposed in this work use thin 2-mm-thick glass mirrors and Alanod films with the reflection coefficient $K_r = 0.95$ [8]. Solar cells of known designs absorb a substantial amount of solar radiation due to a great thickness of glass (4 mm and more) in mirrors and safety shields [9]. On the frontal walls of the Λ-shaped PVMs, either there are no protective glass sheets on the solar cells or, if any, their thickness does not exceed 1.5 mm; therefore, $D \le 0.94$.

As a result, the optical concentration for 12 mirrors reaches $C_{op} = 10.1$.

During the halt time τ of the solar tracking system—a device that tracks the motion of the Sun—the solar radiation reflected by the mirrors displaces across the frontal walls for the distance $b_p = \tau R\omega$, where R is the distance between the frontal wall and the rotational axis of the supporting frame and ω is the angular speed of the Earth's rotation. The tracker controller checks that the reflected radiation covers continuously a surface of the solar cell with a width b_f and partially the photo-selective film, for which purpose the reflection width b_x must exceed the width of the solar cells as $b_x \geq (b_f + b_p)$. The light spot beyond the solar cell array is absorbed by the $TiNO_x$ photo-selective film with a thickness b_p and the radiation absorption coefficient $\beta = 0.94$ [10]. At the back walls of the PVM channels, solar cells are positioned that perform single concentration of the total solar radiation and generate electric power for the auxiliaries of the cogeneration plant.

In double-sided PVMs, flexible SunPower Maxeon solar cells with a size of 0.125 × 0.125 m are used in which the voltage at the maximum power point equals 0.54 V [11]. The base number of solar cells n on the channel walls is found from the condition of maintaining the optimal battery charge voltage at approximately 14.4 V and is $n = 14.4/0.54 = 27$. The solar cell temperature along the channel walls increases along the heat-transfer-fluid path. At a temperature coefficient of voltage k_U and a difference Δt_j between the solar cell temperature j and a standard temperature of 25°C, the idle voltage decreases by $\Delta U_j = k_U \Delta t_j$. The total temperature losses of the voltage in the channels equal $U_t = \sum k_U \Delta t_j$. The total temperature losses of the voltage in the first photovoltaic module downstream the heat-transfer fluid are small; to compensate for these losses, an additional solar cell is integrated into each of the channels of this module. The heat-transfer fluid from the first PMV's channels comes into the channels of the second high-temperature PVM where three solar cells are integrated into each. As a result, the length of the first channel is $L_1 = (n + 1)\, b_f$, and that of the second channel is $L_2 = (n + 3)\, b_f$.

CALCULATING THE TEMPERATURE OF HEAT-TRANSFER FLUIDS AND SOLAR CELLS

The scheme of calculating the heat-transfer-fluid temperatures in the channel with encapsulated solar cells on the frontal and back (facing the Sun) walls is shown in Fig. 2. The heat-transfer fluid with a temperature t_{in} comes into the channel along the 0–x axis; at the channel outlet, the heat-transfer-fluid temperature is t_{out}. The expressions for the heat fluxes radiated by the solar cells, namely, the heat flux q_1 that passes

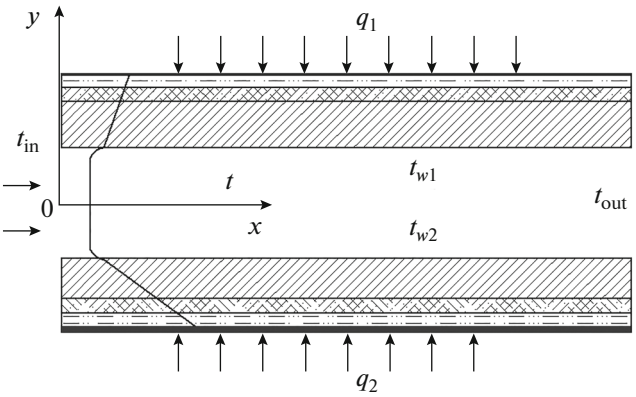

Fig. 2. Scheme of calculating the heat-transfer fluid temperatures in the channels of the solar cell.

through the frontal walls and the heat flux q_2 that passes through the back walls, can be written as:

$$q_1 = \eta_{h1} C_{op} E_d (1 - \eta_{e1});$$

$$q_2 = \eta_{h2} E_d [1 + (E_f / E_d)](1 - \eta_{e2}),$$

where η_{e1}, η_{e2}, η_{h1}, and η_{h2} are experimental coefficients of the electric and thermal efficiency of the solar cells and E_f and E_d are the peak power of the direct and diffuse solar radiation.

The heat release increases at the end of the channel; however, due to the face-to-face arrangement of the frontal walls, the heat radiation from the hotter outlet sections of the channel comes into the inlet sections, which compensates for the increased heat release at the outlet. As a result, the problem of the steady-state heat exchange process to the one-dimensional integral approximation with a uniform distribution of the heat flux over the wall arises. The thermal conductivity along the wall length can be neglected. According to the law of conservation of energy, the equation of the heat balance along the channels can be written in the form [12]

$$(q_1 + q_2) b \mathrm{d}x = c_p G \mathrm{d}t, \tag{3}$$

where c_p and G are the heat capacity and consumption rate of the heat-transfer fluid and t is the heat-transfer-fluid temperature average over the channel cross section.

Equation (3) with separable variables has an analytical solution as:

$$t = t_{in} + \frac{(q_1 + q_2) b x}{c_p G}. \tag{4}$$

The mean integral temperature of the heat-transfer fluid $\bar{t}$ equals

$$\bar{t} = \frac{t_{in} + t_{out}}{2} = t_{in} + \frac{(q_1 + q_2) b L}{c_p G}.$$

Fig. 3. Appearance of a laboratory cogeneration plant.

The heat transfer inside the channels occurs according to Newton–Richman's law [13] as:

$$q_1 = \alpha_1(\overline{t}_{w1} - t); \quad q_2 = \alpha_2(\overline{t}_{w2} - t),$$

where $\overline{t}_{w1}$ and $\overline{t}_{w2}$ are the mean integral temperatures of the walls and α_1 and α_2 are the wall-length average heat-transfer coefficients.

The heat flux through the back wall can be considered by the experimental parameter $\theta = q_2/q_1$. Given this and solving the equation of the thermal conductivity with the boundary conditions of the third kind, we can obtain an expression for calculating the mean integral temperature of the solar cells t_f on the frontal wall as:

$$t_f = t_{\text{in}} + \eta_h C_{\text{op}} E_d (1 - \eta_e) \times \left[\frac{(1+\theta) bL}{c_p G} + \frac{1}{\alpha_1} + \sum \frac{\delta_i}{\lambda_i} \right], \quad (5)$$

where

$$r_1 = \frac{1}{\alpha_1} + \sum \frac{\delta_i}{\lambda_i} \quad (6)$$

is the thermal resistance in the heat flux path (m^2 K/W) and δ_i and λ_i are the thickness (m) and the thermal conductivity (W/(m K)) of the sealing layer, the protective aluminum oxide layer, and the wall.

In plane channels, the heat-transfer coefficient of the fluid under laminar flow is $\alpha_1 \geq 320$ W/(m^2 K); hence, $\frac{1}{\alpha_1} \approx 3.1 \times 10^{-3}$. The resistance $\frac{\delta_i}{\lambda_i}$ (m^2 K/W) of the 0.3-mm-thick KPTD-3 sealant layer with a thermal conductivity of 1.8 W/(m K) is 0.16×10^{-3}, that of the 0.1-mm-thick protective aluminum oxide layer with a thermal conductivity of 2.0 W/(m K) is 0.05×10^{-3}, and the resistance of the 2.0-mm-thick walls of an aluminum alloy with thermal conductivity of 192.0 W/(m K) is 0.01. As a result, the total thermal resistance r_1 between the solar cells and the fluid is 3.31×10^{-3} m^2 K/W.

In [14], results of a study into the influence of the temperature and solar radiation concentration on the efficiency of the Maxeon solar cells are provided. According to the experimental data, graphs of the peak power P were constructed and the value of the coefficient $\eta_e \approx 0.17$ used in Eq. (5) was obtained. The value of the coefficient η_h was found by the data of studies conducted on thermotechnical test benches and a laboratory cogeneration plant, which is represented in Fig. 3.

The optical concentration was varied by changing the tilt angle of the flat mirrors. The temperature of the heat-transfer fluids was controlled by chromel–copel thermocouples within an error of ±3°C, the consumption rate was controlled by rotameters, and the temperature of the solar cells was measured by a UT300A pyrometer within an error of ±11°C. The technological parameters in the flat channel of the linear collector were measured according to the standard method described in [15]. The thermal efficiency coefficient of the laboratory setup was approximately 0.61. The heat losses proved to be high (39%) and increased with the increasing temperature of the solar cells. To reduce the losses, the face-to-face arrangement of the frontal walls with the mutual shielding of the heat radiation is proposed [16, 17]. In the heat-transfer theory, the value of the heat flux q emitted from the hot walls is determined by the Stefan–Boltzmann law as

$$dq = \varepsilon\sigma_0 \left[\left(\frac{T}{100} \right)^4 - \left(\frac{T_0}{100} \right)^4 \right] dF \int_0^{\pi} d\psi, \quad (7)$$

where ε is the emissivity, σ_0 is the Stefan–Boltzmann constant [$\sigma_0 = 5.67 \times 10^{-8}$ W/(m^2 K^4)], T is the temperature of the walls (K), T_0 is the ambient temperature (K), F is the area of the radiating surface (m^2), and ψ is the angle (rad) within which the radiation propagates [18].

In similar systems, the radiation angle of the frontal walls is within the range (0–π); in the Λ-shaped PVMs,

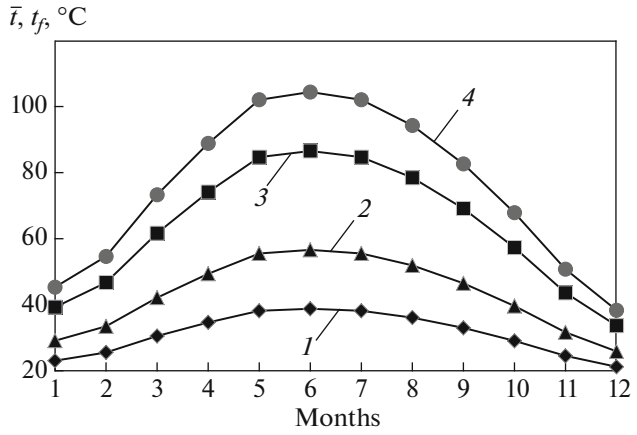

Fig. 4. Mean integral heat-transfer fluid temperatures in (*1*) channel 1 and (*3*) channel 2 and of the solar cells in (*2*) channel 1 and (*4*) channel 2 at $G = 150$ kg/h.

owing to the mutual shielding, the radiation angle equals $\left[0 - \left(\frac{\pi}{2} + \varphi\right)\right]$.

The ratio of energy losses due to radiation ζ in the PVM designs under comparison is $\zeta = \frac{\frac{\pi}{2} + \varphi}{\pi} = 30\%$ at the equal temperature and emissivity of the walls; for the $TINO_x$ photo-selective films, $\varepsilon \approx 0.1$. Moreover, the frontal walls form a semienclosed trough in which the air flow heated by the walls rises by convection, creates additional thermal resistance, and reduces the convective heat losses by approximately 5%. This results in the total heat losses in the innovative PVMs that are 35% lower than the losses of known analogous designs. Given this and considering the results of testing the plant (see Fig. 3), the heat losses are $0.39 \times (1.0 - 0.35) = 0.25$ and, accordingly, the value of the second experimental coefficient in Eq. (5) can be taken as equal to $\eta_h = 0.75$ and, with a certain margin for further calculations, as equal to 0.72.

In the solar tracking system of the optical concentrator, Venture 850 actuators are used with a 55-W DC gear-motor drive that creates a force of up to 3175 kg. The frequency of switching on the tracking system for 15 s is 1 min. Therefore, the total operation time of the electric drive is 7.5 min/h and the energy losses do not exceed 10 W h. The power consumed to pump the antifreezing solution [$c_p \approx 0.9$ W h/(kg K)] by micropumps is approximately 100 W h, that to circulate the water used in the heat exchanger circuit is 120 W h, and that to operate the automatic devices is 50 W h. The total power consumption is 280 W h, i.e., 11% of the overall peak power of the cogeneration system. The expenditure of energy is completely covered by the solar cells that operate at a single solar concentration.

Given the above information, the expression for calculating the mean integral temperatures of the heat-transfer fluids $\bar{t}$ and solar cells t_f can be written in the form

$$\bar{t} = t_{\text{in}} + 4.7E_d \frac{0.66}{G}; \tag{8}$$

$$t_f = t_{\text{in}} + 4.7E_d\left(\frac{0.66}{G} + 0.0033\right). \tag{9}$$

In Fig. 4, the results calculated at $t_{\text{in}} \approx 15$°C are represented in the form of graphs considering the data on the climatic conditions in Almaty, according to which $E_d \approx 1150$ W/m^2 in June. At the consumption rate $G \approx 150$ kg/h, for the first channel, $\bar{t}_1 \approx 15 + 4.7 \times 1150 \frac{0.66}{150} \approx 39$°C and $t_{f1} \approx 15 + 4.7 \times 1150\left(\frac{0.66}{150} + 0.0033\right) \approx 57$°C. The difference between the temperatures of the solar cells and the heat-transfer fluid is $57 - 39 \approx 18$°C. The heat-transfer-fluid temperature at the first channel outlet equals $t_{\text{out}1} = 2\bar{t}_1 - t_{\text{in}} = 2 \times 39 - 15 \approx 63$°C. For the second channel, $\bar{t}_2 \approx 63 + 4.7 \times 1150\frac{0.66}{150} \approx 87$°C and $t_{f2} \approx 63 + 4.7 \times 1150\left(\frac{0.66}{150} + 0.0033\right) \approx 105$°C. The temperature at the second channel outlet equals $t_{\text{out}\,2} = 2\bar{t}_2 - t_{\text{in}} = 2 \times 87 - 63 \approx 111$°C. At the heat-transfer-fluid consumption rate $G \approx 150$ kg/h, the temperature of the solar cells at midday exceeds the standard-operation temperature; therefore, the control system promptly increases the heat-transfer-fluid consumption rate to $G \approx 180$ kg/h.

Consequently, the connection of the PVMs in series allows for maintaining high electric efficiency of the solar cells in the first channel and simultaneously achieving a high heat-transfer-fluid temperature at the second channel outlet at equal dimensions of the channels, which makes the solar cell encapsulating technology simpler.

CALCULATION OF THE PHOTOVOLTAIC MODULE PERFORMANCE

The output–input power balance in the PVM channels connected in series with solar cells placed on the walls and a photo-selective film is written in the form

$$\left.\begin{aligned} &2(n+1)S_f E_d\left[\left(C_{\text{op}} + 1 + \frac{E_f}{E_d}\right)\right. \\ &\left. + \frac{b_p}{b_f}\beta\left(C_{\text{op}} + 1 + \frac{E_f}{E_d}\right)\right] = \frac{Q_1}{\eta_{h1}} + P_{j1} + P_{i1}; \\ &2(n+3)S_f E_d\left[\left(C_{\text{op}} + 1 + \frac{E_f}{E_d}\right)\right. \\ &\left. + \frac{b_p}{b_f}\beta\left(C_{\text{op}} + 1 + \frac{E_f}{E_d}\right)\right] = \frac{Q_2}{\eta_{h2}} + P_{j2} + P_{i2}, \end{aligned}\right\} \tag{10}$$

Table 1. Parameters of the cogeneration plant

Parameter	Month											
	1	2	3	4	5	6	7	8	9	10	11	12
W_d, kW h/m^2	37	47	89	137	191	212	203	171	116	68	40	28
W_f, kW h/m^2	17	23	34	44	46	45	45	45	41	24	15	15
$\sum W_{dD}$, kW h/m^2	1.5	2.2	3.7	5.3	6.6	7.2	6.6	5.7	4.5	3.1	1.9	1.3
E_d, kW/m^2	0.39	0.51	0.75	0.95	1.12	1.15	1.12	1.02	0.87	0.68	0.46	0.3
x'	0.46	0.49	0.38	0.32	0.24	0.2	0.2	0.26	0.34	0.35	0.37	0.5
N_d, h	3.85	4.31	4.93	5.58	5.89	6.26	5.89	5.59	5.17	4.56	4.13	4.3
τ_m, h	92	91	118	145	171	185	181	168	134	100	87	95

W_d and W_f are the direct and diffuse solar radiation; $\sum W_{dD}$ is the sum of the direct solar radiation per day onto a horizontal panel, and $x' = W_f / W_d$.

where S_f is the area of a solar cell; Q_1 and Q_2 are the available heat power of channels 1 and 2; η_{h1} and η_{h2} are the heat efficiency coefficients of channels 1 and 2; P_{j1} and P_{j2} are the peak electric power of the solar cells with sun radiation concentration; and P_{i1} and P_{i2} are the peak electric power of the solar cells without sun radiation concentration.

To simplify the calculations, the mean annual value $E_f / E_d = 0.3$ can be adopted. Upon transformations and substitution into (10) of the measured technological parameters of the developed design, the analytical expressions for calculating the average monthly peak electric P and thermal Q power (kW) of the cogeneration plant take the form

$$P = P_1 + P_2 = 2.9E_d; \quad (11)$$

$$Q = Q_1 + Q_2 = 11.7E_d. \quad (12)$$

To determine the average monthly performance of the system, one has to know the number of the hours with the solar radiation intensity E_d. In Table 1, the climate data are presented [19] according to which the average monthly technological variables of the cogeneration plant were found.

According to the data of the table, the average annual direct solar radiation is $E_{d\,\mathrm{av}} = 0.78$ kW/m^2; hence, the average annual peak power of the cogeneration plant will be $W_{d\,\max} = (P+Q)_{\mathrm{av}} = 14.6\ E_{d\,\mathrm{av}} = 11.4$ kW/m^2. The maximum daily peak solar radiation hits the mirror surfaces from 12 a.m. to 1 p.m. each month and equals

$$E_{d\,\max} = \frac{W_{d\,\max}}{\cos(\varphi_{\mathrm{IN}} \pm \delta')},$$

where φ_{IN} is the latitude (deg) of the installation site and δ' is the solar declination (deg).

The number of the hours per day with the maximum radiation intensity N_d can be found by the climate data [19] considering the total average monthly daytime radiation. The number of active hours per month is $\tau_m = n_m N_d$, where n_m is the number of bright days per month.

For the cogeneration plant prototype with $\varphi = 50°$ and the focal distance $f = 1.7$, the projection of the mirrors on the x-axis equals $x_N = 1.6$ m and the total length of the mirrors for two PVMs considering the cosine losses and a distance between the solar cells of 0.001 m is $l \approx (2n + 4) \times 0.125$; hence, the area of the mirrors' optical aperture $S_a = 2x_N l = 24.2$ m^2. The average monthly specific output (kW h/m^2) is $O_P = 2.9\frac{E_d}{S_a}\tau_m = 0.12E_d\tau_m$ for electrical energy and $O_Q = 11.7\frac{E_d}{S_a}\tau_m = 0.47E_d\tau_m$ for heat energy.

In Fig. 5, the graph of the average monthly specific output of the cogeneration plant prototype is shown for

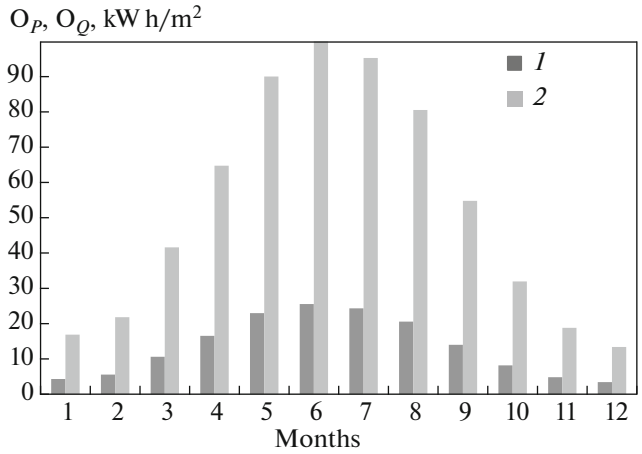

Fig. 5. Average monthly specific (*1*) electricity and (*2*) heat output of the cogeneration plant.

the latitude of Almaty. The annual specific electricity output is $\sum O_P = 160$ kW h/m^2 and the annual specific thermal power output is $\sum O_Q = 629$ kW h/m^2. For comparison, we should note that, at a lower southern latitude of 37° in California, the specific electrical output of Cogenra Solar plants, which are the closest analogues to the plant in question, is 168 kW h/m^2 and their specific thermal energy output is 657 kW h/m^2.

COGENERATION PLANTS FOR HOT WATER SUPPLY

According to the requirements of the hot water supply standard, per capita daily consumption of water with a temperature of 55°C is 120 dm^3 [20]. Given the heat losses, such figures can be achieved under efficient heat exchange between the heat-transfer fluids in the heat exchanger at an outlet temperature of 70°C at least. The heat losses in the section from the heat exchanger to the heat-insulated container were reduced by approximately 10% by eliminating long flexible pipelines. According to Eq. (12), the equation of the peak power balance during the transmission of the energy from the heat-transfer fluids to the consumed process water has the form

$$0.9\times11.7E_d = c_pG_2(t_2 - t_1), \qquad (13)$$

where t_1 and t_2 are the water temperatures (°C) at the heat exchanger inlet and outlet and G_2 is the water consumption rate (kg/h).

At the preset level of heating the process water $\Delta t = 50°$, the average monthly consumption per hour G_2 is calculated by Eq. (13). Based on the data of Table 1, the number of active hours per day N_d is found and then, the average monthly mass M of the process water accumulated during a day for hot water supply is calculated as $M = G_2N_d$. Figure 6 shows the graph of the average monthly consumption rate per hour and the total daily amount of process water heated to 65°C.

To provide a farmer family of five persons with hot water considering their economic activity, the volume of water $V = 850$ dm^3/day is required. The cogeneration plant completely meets the hot water demand from May to September (see Fig. 6); in the other months, additional heat energy sources are needed, such as boilers or diesel generators.

The transportation of hot water under direct conversion of heat energy is affected using thermosiphoning in the closed heat-exchanger loop that includes an insulated container with water. The required level and temperature of the water in the container are maintained during the day by a controller. The water for the hot water supply is withdrawn from the upper point of the container and the cold water is refilled at the lower point; due to this, the maximum difference between the mean temperatures in the heat exchanger and the return

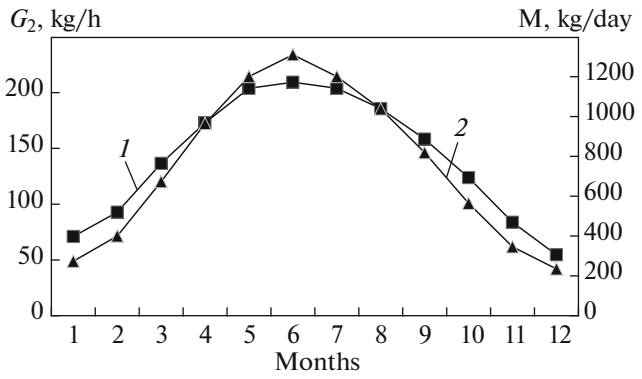

Fig. 6. Schedule of the (*1*) hourly consumption and (*2*) storage of the daily amount of heated water.

pipeline is achieved. After the sunset, the cold-water inflow is stopped for the time the container is emptied.

During the heating, the density of water decreases and, as a consequence of the difference between the mass of the water in the heat exchanger and that in the return pipeline, natural circulation of water occurs with the dynamic differential pressure

$$\Delta p = gh(\rho_{r.p} - \rho_h), \qquad (14)$$

where g is the acceleration of gravity (9.81 m/s^2), h is the distance (m) between the central point of the heat exchanger and the insulated container (see Fig. 1), and ρ_h and $\rho_{r.p}$ are the length-average densities of water (kg/m^3) in the heat exchanger and the return pipeline.

The density of the water in the heat exchanger at a mean temperature of 50°C equals 988.1 kg/m^3 and that in the return pipeline is 999.5 kg/m^3 at a mean temperature of 18°C [21]. At the mean height in the plant prototype $h = 4.5$ m, according to Eq. (14), the maximum dynamic differential pressure will be $\Delta p = 500$ N/m^2.

Part of the heat energy generated by the solar cells is converted into mechanical energy when the heated water is transported in the circulation circuit with a length L' and a diameter d. The friction resistance F_1 under laminar flow of the fluid is determined by the expression

$$F_1 = \frac{\xi L'u^2}{2d},$$

where $\xi = \frac{64}{\mathrm{Re}}$ is the friction resistance coefficient and u is the velocity of the process water in the heat exchanger.

For a prototype with $L = 27$ m, $d = 0.15$ m, and the Reynolds number Re ≤ 1500, the friction resistance is $F_1 \le 20$ N/m^2 and $\xi \le 0.26$. When the fluid flows through turns and along convergent and divergent sections of the circulation circuit, local resistances $F_2 \le 25$ N/m^2 occur.

As a result, the dynamic differential pressure Δp compensates for all hydraulic resistances and ensures intensive natural hot water circulation.

Under varying solar radiation intensity over the day, the specified performance of cogeneration systems is maintained by adjusting the position of the mirrors, the heat-transfer-fluid consumption rates, and the refilling of the cold-water circuit. Special attention is paid to the development of the algorithms and corresponding programs for controlling the technological process and selecting efficient and reliable actuators.

Based on the experience of manufacturing laboratory facilities using components acquired on-line, we can estimate the production costs of a cogeneration plant prototype with an aperture area of 25 m^2 at approximately \$4900; hence, the cost of the average annual installed capacity may be estimated at 0.43 \$/W. For comparison, the cost of the installed capacity of the closest analogue of the plant in question, a Cogenra Solar system, is 2.34 \$/W. According to the incentive rate of selling the electrical energy generated using renewable energy sources [22], the selling price of electrical energy is 0.108 \$/(kW h). The annual revenue from selling the electric energy generated by the plant in question will be \$432. With a thermal energy rate for remote localities of 0.034 \$/(kW h), the annual revenue from selling electric energy is estimated at \$534. As a result, from selling electrical and thermal energy, the consumer will earn a revenue of \$966. In this case, the expenses of the buyer of the plant will pay off in 5 years. Compared with conventional solar panels and hybrid solar systems, the pay-off period of the solar systems is reduced more than twofold. In remote localities for which, in fact, the cogeneration systems are developed, the electrical and thermal energy rates are considerably higher; therefore, the pay-off period is reduced to 3–4 years.

CONCLUSIONS

(1) Using the Inventor 10 software, the design of linear photovoltaic modules has been optimized. Analytical expressions for calculating the working components of the optical concentrator with the face-to-face positioned frontal walls with silicon solar cells in the focal spot have been derived for the first time. The use of high-quality materials and components available on the market allows for the construction of light and reliable supporting frames for flat mirrors and for optical efficiency of the concentrator of approximately 0.83 to be achieved.

(2) Owing to the mutual shielding of the heat radiation from the frontal walls and formation of a protective thermal layer in the trough-shaped channels, the heat losses have been reduced by 35%, the coefficient of thermal efficiency of the Λ-shaped photovoltaic modules has been increased accordingly, and the temperature of the heat-transfer fluids in the channels could be increased to 85°C.

(3) The technology (know-how) developed for encapsulating the solar cells on the frontal walls with a low thermal resistance and maintaining the collinearity between the former has allowed for a considerable increase in the reliability and efficiency under a high photocurrent.

(4) The complicated engineering problem of transporting electrical and thermal energy from movable photovoltaic modules to a fixed energy storage system has been solved using patented engineering solutions and technological know-how.

(5) Considering the conversion of the solar radiation intensity into that at equal geographic latitudes, the specific output of the innovative cogeneration systems exceeds that of known analogues.

(6) The calculations show an almost twofold increase in the temperature of the heat-transfer fluids compared with analogous plants under identical operating conditions of the photovoltaic modules. This increases the intensity of the heat-transfer processes in the heat exchanger and has allowed for the first time for the efficient transportation of heat energy to the storage system under natural flow of the consumed process water in the circulation circuit.

(7) Given the selling rates for energy generated from renewable sources currently existing in Kazakhstan, the pay-off period of the innovative cogeneration plants is estimated at 5 years. The solar panels with silicon solar cells produced in Kazakhstan or Russia, pay off over 10–12 years.

(8) A distinguishing feature of the cogeneration plants with Λ-shaped photovoltaic modules is that the amount of the generated thermal energy exceeds the amount of the generated electrical energy almost threefold. At a considerably lower cost of thermal energy, the economic revenue from selling it proves to be higher than that from selling electricity. The rates for electric and thermal energy are increasing every year while the market prices of solar system components are decreasing by 4%; therefore, the business of manufacturing and installing cogeneration systems has good prospects.

REFERENCES

1. T. T. Chow, "A review on photovoltaic/thermal hybrid solar technology," Appl. Energy **87**, 365–379 (2010). https://doi.org/10.1016/j.apenergy.2009.06.037
2. J. A. Duffie and W. A. Beckman, *Solar Engineering of Thermal Processes*, 3rd ed. (Wiley, Hoboken, NJ, 2006).
3. A. Kribus, D. Raftori, G. Mittelman, A. Hirshfeld, and A. Dayan, "A miniature concentrating photovoltaic end thermal system," Energy Convers. Manage. **47**, 3582–3590 (2006). https://doi.org/10.1016/j.enconman.2006.01.013

4. J. S. Coventry, "Performance of a concentrating photovoltaic/thermal solar collector," Sol. Energy **78**, 211–222 (2005). https://doi.org/10.1016/j.solener.2004.03.014

5. *Cogenra's 'Hybrid' Solar System Captures 80% of the Sun's 111.* https://www.treehugger.com › renewable-energy. Accessed May 24, 2019.

6. A. G. Nesterenkov, P. A. Nesterenkov, and L. A. Nesterenkova, "The method of converting solar radiation into electrical and thermal energy and the plant for implementing the method," RK Patent No. 30003, Baza Patent Kaz. (2015).

7. P. A. Nesterenkov, A. G. Nesterenkov, and L. A. Nesterenkova, "Fundamentals of designing hybrid concentrator solar systems," in *Proc. 12th Int. Conf. on Concentrator Photovoltaics (CPV-12), Freiburg, Germany, April 25–27, 2016* (American Inst. of Physics, 2016).

8. https://www.alanod.com. Accessed February 25, 2019.

9. L. C. Chea, H. Hakansson, and B. Karlsson, "Performance evaluation of new two axes tracking PV-thermal concentrator," Am. J. Civ. Eng. Archit. **7**, 1485–1493 (2013). https://doi.org/10.17265/1934-7359/2013.12.002

10. *Almeco-Tinox Solar. Tinox Energy.* http://www.almecogroup.com/en/pagina/16-solar

11. Z. S. Judkins, K. W. Johnston, C. Almy, R. J. Linderman, B. Wares, N. A. Barton, M. Dawson, and J. Peurach., *Performance Results of a Low-Concentration Photovoltaic System Based on High Efficiency Back Contact Cells*, SunPower Corporation Report (2010).

12. M. A. Mikheev and I. M. Mikheeva, *Fundamentals of Heat Transfer* (Energiya, Moscow, 1977) [in Russian].

13. V. P. Isachenko, V. A. Osipova, and A. S. Sukomel, *Heat Transfer* (Energiya, Moscow, 1969; Mir, Moscow, 1969).

14. P. A. Nesterenkov, L. A. Nesterenkova, and A. G. Nesterenkov, "Cogeneration solar systems with concentrators of solar radiation," in *Handbook of Research on Renewable Energy and Electric Resources for Sustainable Rural Development* (IGI Global, Hershey, PA, 2018), pp. 230–254. https://doi.org/10.4018/978-1-5225-3867-7.ch010

15. V. A. Osipova, *Experimental Investigation of Heat Exchange Processes: Study Aid* (Energiya, Moscow, 1979) [in Russian].

16. A. G. Nesterenkov, P. A. Nesterenkov, and L. A. Nesterenkova, "A method of converting solar radiation and a cogeneration plant for implementing the method," RK Patent No. 33513, Baza Pat. Kaz. (2018).

17. P. A. Nesterenkov and V. V. Kharchenko, "Thermo physical principles of cogeneration technology with concentration of solar radiation," in *Proc. 2nd Int. Conf. on Intelligent Computing & Optimization (ICO 2019), Koh Samui, Thailand, Oct. 3–4, 2019* (Springer-Verlag, Cham, 2019), Vol. 1, pp. 117–128.

18. A. G. Blokh, Yu. A. Zhuravlev, and L. N. Ryzhkov, *Radiative Heat Transfer: Handbook* (Energoatomizdat, Moscow, 1991) [in Russian].

19. *USSR Climate Handbook, Series 3: Multi-Year Data*, Vol. 1–6, Iss. 18: *Kazakh SSR*, (Gidrometeoizdat, Moscow, 1989), Book 1 [in Russian].

20. *Water Consumption per Person per Day.* https://hitropop.com/voda/normy/potreblenie-v-sutki.html

21. *Thermophysical Properties of Substances: Handbook*, Ed. by R. B. Vargaftik (Gosenergoizdat, Moscow, 1956) [in Russian].

22. *Tariffs on Renewable Energy Sources*. http://astanasolar.kz/ru/news/utverzhdeny-tarify-na-vozobnovlyaemye-istochniki-energii

Translated by O. Lotova